VELOCITY KINEMATIC CONTROLLER DESIGN FOR AN INDUSTRIAL MANIPULATOR WITH A PALLETIZING CONFIGURATION

THIẾT KẾ BỘ ĐIỀU KHIỂN ĐỘNG HỌC VẬN TỐC CHO ROBOT CÔNG NGHIỆP ĐƯỢC TÁI CẤU HÌNH THEO DẠNG PALLETIZING

Trong Hieu Luu, Quang Hieu Ngo*, Nguyen Bao Vo, Duc Thinh Le

College of Engineering, Can Tho University, Vietnam

*Corresponding author: nqhieu@ctu.edu.vn

(Received: July 04, 2025; Revised: August 08, 2025; Accepted: August 29, 2025)

DOI: 10.31130/ud-jst.2025.23(9A).361

Abstract - This paper presents the design of a velocity kinematic controller for a 6-degree-of-freedom Motoman industrial robotic arm applied in palletizing tasks. To simplify the control system and maintain stability during pick-and-place operations, the original structure of the robotic arm is reconfigured into a 4-degree-of-freedom system by fixing some joints. Additionally, the end-effector is constrained to remain perpendicular to the working plane throughout operation. A new kinematic model is developed based on the adjusted hardware structure, in which the end-effector's velocity is computed using the Jacobian matrix. To evaluate the proposed control method, three different trajectories are defined: linear, circular, and clover-shaped paths. Both simulation and experimental tests are conducted, focusing on analyzing the variation in end-effector velocity. The results demonstrate that, the proposed system can accurately guide the end-effector along the desired paths, confirming the effectiveness and practical applicability of the approach in industrial robotic control for palletizing tasks.

Key words - Robot palletizing; industrial manipulator; velocity kinematic control; Jacobian matrix

Tóm tắt - Nghiên cứu này trình bày thiết kế bộ điều khiển động học vận tốc cho tay máy công nghiệp Motoman 6 bậc tự do trong ứng dụng xếp hàng lên pallet. Để đơn giản hóa hệ thống điều khiển và đảm bảo ổn định trong thao tác gắp thả, cấu trúc ban đầu của tay máy được điều chỉnh thành tay máy 4 bậc tự do bằng cách cố định một số khớp, đồng thời giữ cho khớp cuối luôn vuông góc với mặt phẳng làm việc. Mô hình động học được xây dựng lại tương ứng, với vận tốc khớp cuối được tính thông qua ma trận Jacobian. Ba dạng quỹ đạo gồm đường thẳng, đường tròn và đường hình cỏ ba lá được thiết lập nhằm kiểm chứng hiệu quả điều khiển. Cả mô phỏng và thực nghiệm đều được thực hiện, tập trung phân tích biến thiên vận của khớp cuối. Kết quả cho thấy, hệ thống đề xuất có khả năng điều khiển khớp cuối di chuyển theo quỹ đạo một cách chính xác, minh chứng cho tính hiệu quả và ứng dụng thực tiễn trong điều khiển robot công nghiệp.

Từ khóa - Robot palletizing; robot công nghiệp; điều khiển động học vận tốc; ma trận Jacobian

1. Introduction

In the field of industrial automation, pick-and-place operations are among the most common and highly applicable tasks, particularly in production lines, packaging, and product sorting. To meet the requirements for speed, accuracy, and high repeatability, palletizing-type industrial robotic systems have been widely deployed in practice. These systems enable robots to automatically perform the stacking of goods onto pallets according to predefined rules or optimized criteria specific to operational demands.

Globally, research on trajectory planning algorithms for palletizing robots has been systematically reviewed in [1]. Specifically, stacking strategies based on heuristics have been investigated to optimize the pick-and-place process for objects of varying sizes [2]. Additionally, optimizing the motion path of the end-effector has garnered significant attention to enhance operational efficiency [3], while safety aspects concerning human-robot collaboration have also been addressed in [4]. Notably, study [5] presents techniques for optimizing motion time to improve speed and efficiency in pick-and-place operations.

In Vietnam, research on industrial robots is also attracting considerable interest from various research groups. From this, the authors in [6] proposed a robust control solution by applying a sliding mode controller combined with neural networks to enhance resistance against external disturbances. Concurrently, studies such as [7] have analyzed the dynamics and optimized the structure of palletizing robots to design and manufacture systems suitable for stacking goods onto pallets. However, due to limitations in hardware investment costs, domestic research often faces difficulties in experimental implementation on modern industrial robot systems. Therefore, leveraging and reconfiguring available hardware platforms is a reasonable approach, both cost-effective and efficient for research purposes.

In this study, we propose a control solution for palletizing-type industrial robots by reconfiguring the 6-degree-of-freedom Motoman robot, in which several joints are locked to reduce unnecessary degrees of freedom for the palletizing task, thereby simplifying the control model and enhancing operational stability.

2. Method

2.1. Kinematic model of the palletizing industrial robot

2.1.1. Forward kinematics

The robot utilized in this study is a palletizing-type industrial robot with four degrees of freedom, modified from the original 6-degree-of-freedom Motoman K3

industrial robot (Figure 1a). For palletizing applications, the robot requires the first three joints (joints 1, 2, and 3) for positioning, while the final joint (joint 6) serves to orient the end-effector such that it remains perpendicular to the working plane. To achieve this, the research team fixed two intermediate joints (joints 4 and 5) using a flexible joint. The modification process involved removing two unnecessary rotary joints and adding an auxiliary link to enhance the robot's lifting and grasping capabilities.

The Cartesian coordinate system of the robot in space is established as shown in Figure 1a, and the simulation coordinate system is similarly depicted. Figure 1b illustrates the control cabinet system, which includes a Siemens S7-1200 PLC and Servopack SGDA drivers, responsible for generating control pulses for the AC servo motors via the TIA Portal software on a computer. Based on this coordinate system, the Denavit-Hartenberg (DH) parameter table for the robot is constructed as shown in Table 1. According to Table 1, the fourth joint is a flexible joint, whose movement is controlled through the adjacent second and third joints.

Table 1. *DH Parameters of the robot*

Joint	a_i	α_i	d_i	θ_i
1	150	π	384	$-\pi < \theta_1 < \pi$
2	295	0	0	$-\frac{\pi}{3} < \frac{\pi}{2} + \theta_2 < \frac{\pi}{3}$
3	444	0	0	$-\frac{\pi}{3} < -\frac{\pi}{2} + \theta_3 < \frac{\pi}{3}$
4	0	$-\pi$	0	$-\theta_3 - \theta_2$
5	0	0	-80	$-\frac{3\pi}{2} < \theta_5 < \frac{3\pi}{2}$

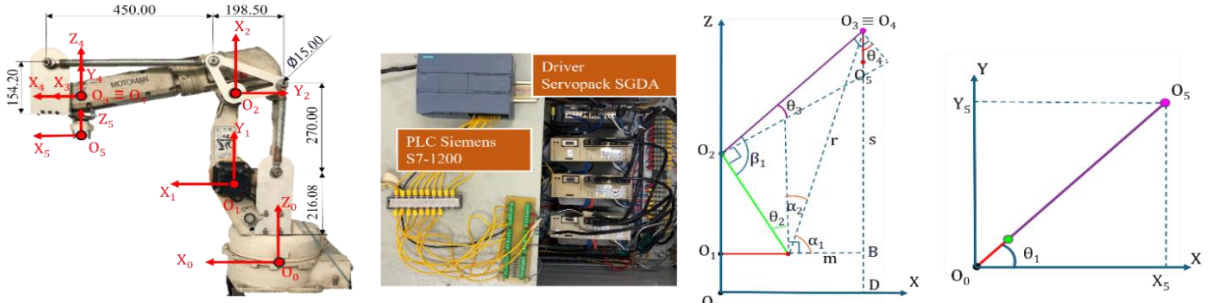

Figure 1. *The Motoman industrial robot redesigned for Palletizing applications*

Where:

- θ_i is the rotation angle about the Z_{i-1} axis from x_{i-1} to x_i,
- α_i is the rotation angle about the Z_{i-1} axis from z_i to x_i,
- a_i is the distance between two Z_{i-1} axes along x_i,
- d_i is the distance along Z_{i-1} between two coordinate frames.

Based on these definitions, the transformation matrix for each link of the industrial manipulator is expressed as follows:

$$A_i = \begin{bmatrix} 0 & R_i^0 & 0 & D_i^0 \\ 0 & 0 & 0 & 1 \end{bmatrix} \quad (1)$$

$$A_n^0 = A_0 \cdot A_1 \cdot \ldots . A_n \quad (2)$$

Where $0 < i < n$

2.1.2. Inverse kinematics

In pick-and-place and palletizing applications, solving the inverse kinematics problem is essential to determine the joint angles corresponding to the desired position and orientation of the end-effector. This enables the manipulator to accurately compute control parameters to move the end-effector to the required position within the workspace. Solving this problem also provides the basis for determining appropriate motion trajectories, ensuring smooth end-effector movement between operation points, while adhering to mechanical limits and avoiding collisions during operation.

In this study, the robot's inverse kinematics is established using geometric methods with side and top views (Figure 1b and Figure 1c), as illustrated below:

Based on the robot's projection in space, the inverse kinematics equations for each joint are described according to [8] as follows:

$$\theta_1 = \tan^{-1}\left(\frac{y_c}{x_c}\right) \quad (3)$$

$$s = z_c + d_5 - d_1 \quad (4)$$

$$m = \sqrt{{x_c}^2 + {y_c}^2} - a_1 \quad (5)$$

$$r = \sqrt{s^2 + m^2} \quad (6)$$

$$\beta_1 = \cos^{-1}\left(\frac{-r^2 + {a_2}^2 + {a_3}^2}{2 \cdot a_2 \cdot a_3}\right) \quad (7)$$

$$\theta_3 = \beta_1 - \frac{\pi}{2} \quad (8)$$

$$\alpha_1 = \tan^{-1}\left(\frac{s}{m}\right) \quad (9)$$

$$\alpha_2 = \frac{\pi}{2} - \alpha_1 \quad (10)$$

$$\theta_2 = \cos^{-1}\left(\frac{{a_3}^2 + {a_2}^2 + r^2}{2 \cdot a_2 \cdot r}\right) - \alpha_2 \quad (11)$$

$$\theta_4 = -\theta_3 - \theta_2 \quad (12)$$

2.2. Velocity kinematics of the Palletizing robot

In the analysis and control of industrial robots, velocity kinematics serves as a bridge between the geometric kinematic model and motion control problems. Unlike forward kinematics, which describes the relationship between joint angles and the position and orientation of the end-effector, velocity kinematics focuses on the relationship between joint velocities and the linear and

angular velocities of the end-effector in the workspace.

To describe this relationship, the Jacobian matrix is used as a mathematical tool linking joint space and task space. The forward Jacobian allows calculation of the end-effector's velocity from joint velocities, supporting trajectory control. Conversely, the inverse Jacobian helps determine the required joint velocities to achieve the desired end-effector velocity. In general, the Jacobian matrix in this study is described as follows:

$$v = J(\theta).\dot{\theta} \tag{13}$$

$$v = \begin{bmatrix} J_v \\ J_\omega \end{bmatrix} \begin{bmatrix} \dot{\theta}_1 \\ \dot{\theta}_2 \\ \dot{\theta}_3 \\ \dot{\theta}_4 \\ \dot{\theta}_5 \end{bmatrix} \tag{14}$$

$$\begin{bmatrix} \dot{x} \\ \dot{y} \\ \dot{z} \\ \omega_x \\ \omega_y \\ \omega_z \end{bmatrix} = \begin{bmatrix} J_{11} & J_{12} & J_{13} & J_{14} & J_{15} \\ J_{21} & J_{22} & J_{23} & J_{24} & J_{25} \\ J_{31} & J_{32} & J_{33} & J_{34} & J_{35} \\ J_{41} & J_{42} & J_{43} & J_{44} & J_{45} \\ J_{51} & J_{52} & J_{53} & J_{54} & J_{55} \\ J_{61} & J_{62} & J_{63} & J_{64} & J_{65} \end{bmatrix} \cdot \begin{bmatrix} \dot{\theta}_1 \\ \dot{\theta}_2 \\ \dot{\theta}_3 \\ \dot{\theta}_4 \\ \dot{\theta}_5 \end{bmatrix} \tag{15}$$

In this study, the robot consists entirely of rotary joints; thus, the linear velocity components $\boldsymbol{J_v}$ and angular velocity components $\boldsymbol{J_\omega}$ in the matrix are redefined as follows:

$$\begin{bmatrix} J_{11} \\ J_{21} \\ J_{31} \end{bmatrix} = R_1^0 \begin{bmatrix} 0 \\ 0 \\ 1 \end{bmatrix} \times (d_5^0 - d_0^0) \tag{16}$$

$$\begin{bmatrix} J_{12} \\ J_{22} \\ J_{32} \end{bmatrix} = R_2^0 \begin{bmatrix} 0 \\ 0 \\ 1 \end{bmatrix} \times (d_5^0 - d_1^0) \tag{17}$$

$$\begin{bmatrix} J_{13} \\ J_{23} \\ J_{33} \end{bmatrix} = R_3^0 \begin{bmatrix} 0 \\ 0 \\ 1 \end{bmatrix} \times (d_5^0 - d_2^0) \tag{18}$$

$$\begin{bmatrix} J_{14} \\ J_{24} \\ J_{34} \end{bmatrix} = R_4^0 \begin{bmatrix} 0 \\ 0 \\ 1 \end{bmatrix} \times (d_5^0 - d_2^0) \tag{19}$$

$$\begin{bmatrix} J_{15} \\ J_{25} \\ J_{35} \end{bmatrix} = R_5^0 \begin{bmatrix} 0 \\ 0 \\ 1 \end{bmatrix} \times (d_5^0 - d_2^0) \tag{20}$$

$$J_\omega = \begin{bmatrix} R_0^0 \begin{bmatrix} 0 \\ 0 \\ 1 \end{bmatrix} & R_1^0 \begin{bmatrix} 0 \\ 0 \\ 1 \end{bmatrix} & R_2^0 \begin{bmatrix} 0 \\ 0 \\ 1 \end{bmatrix} & R_3^0 \begin{bmatrix} 0 \\ 0 \\ 1 \end{bmatrix} & R_4^0 \begin{bmatrix} 0 \\ 0 \\ 1 \end{bmatrix} \end{bmatrix} \tag{21}$$

Thus, the inverse Jacobian matrix is implemented as follows:

$$\begin{bmatrix} \dot{\theta}_1 \\ \dot{\theta}_2 \\ \dot{\theta}_3 \\ \dot{\theta}_4 \\ \dot{\theta}_5 \end{bmatrix} = \begin{bmatrix} J_v \\ J_\omega \end{bmatrix}^{-1} \begin{bmatrix} \dot{x} \\ \dot{y} \\ \dot{z} \\ \omega_x \\ \omega_y \\ \omega_z \end{bmatrix} \tag{22}$$

3. Results

To evaluate the feasibility of the proposed control method and the newly integrated mechanical configuration, the research team conducted experiments to assess the accuracy, smoothness, flexibility, and responsiveness of the hardware system. Specifically, the robot was programmed to follow three motion trajectories of increasing complexity, including linear, circular, and clover-shaped paths. Each trajectory was repeated three times to ensure the reliability of the results.

3.1. Experiment 1: Linear trajectory

Experiment 1 evaluates the end-effector's control capability when the trajectory is a straight line. The start and end coordinates in the workspace are set as $A = [590\ 0\ 599]^T$ and $B = [590\ 400\ 599]^T$ (units: mm), respectively.

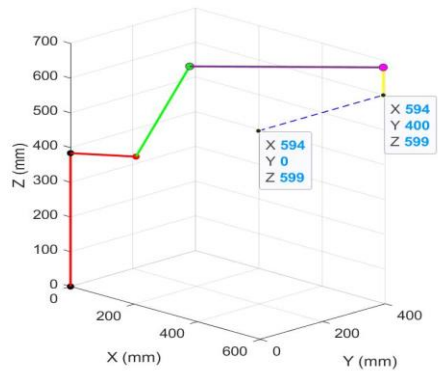

a. Linear trajectory simulation

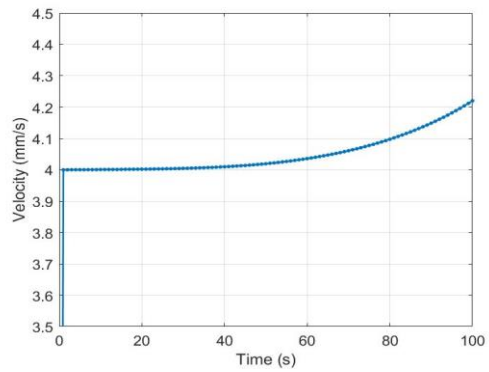

b. End-effector velocity variation chart (image adjusted)

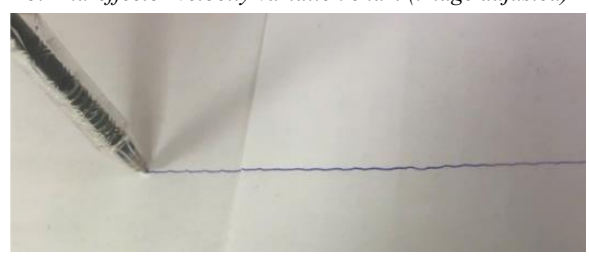

c. Actual linear motion of the end-effector

Figure 2. *Linear trajectory of the end-effector*

To ensure smooth end-effector movement, the trajectory is divided into 100 segments, with each segment executed in 1 second. The simulation results are presented in Figure 2a, while Figure 2b shows the velocity-time graph at the end point. Observations indicate that the end-effector's velocity gradually increases and reaches its maximum at the endpoint, due to the final joint's movement away from the manipulator's center.

Figure 2c illustrates the actual motion results of the robot.

After three repetitions, the end-effector successfully followed the desired trajectory. However, due to the division into 100 small segments with 1-second intervals, the overall motion still exhibits limited smoothness. The straight-line trajectory records an error of $d = \pm 20\ mm$. The average velocity during execution is approximately $v_{tb} = 4.12\ mm/s$.

3.2. Experiment 2: circular trajectory

Experiment 2 was conducted to assess the robot's end-effector control capability in circular trajectory tracking. The center of the circle is set at $I = [590\ 0\ 599]^T$ with a radius $R = 100\ mm$. To ensure continuous and accurate motion, the trajectory is divided into 360 segments, with a 1-second interval between segments.

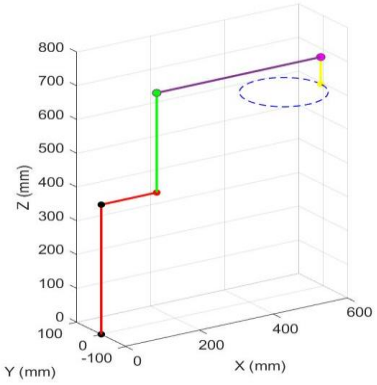

a. Circular trajectory simulation

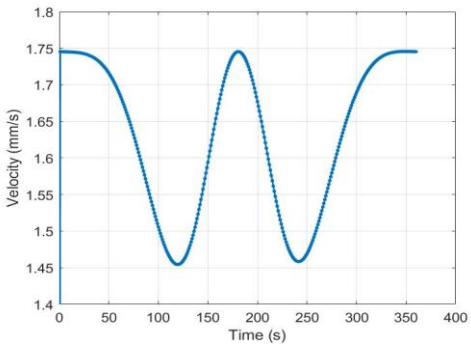

b. End-effector velocity variation chart for circular trajectory (image adjusted)

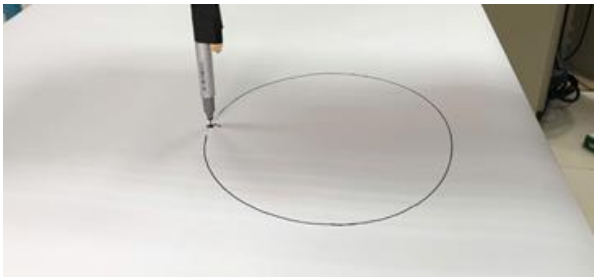

c. Actual circular motion of the end-effector

Figure 3. *Circular trajectory of the end-effector*

Simulation results are shown in Figure 3a, while the end-effector velocity chart during trajectory execution is presented in Figure 3b. The results indicate that the velocity tends to increase as the end-effector moves farther from the manipulator's center and decreases as it approaches the origin, reflecting the dependence of end-effector velocity on its geometric position in the workspace.

The actual robot motion during circular trajectory execution is illustrated in Figure 3c. After three repetitions, the control system ensures that the end-effector closely follows the desired trajectory; however, similar to the previous experiment, the motion smoothness remains limited due to relatively long intervals between steps. The circular trajectory records a radius error of $R = \pm 15\ mm$. The average velocity during execution is approximately $v_{tb} = 2.15\ mm/s$.

3.3. Experiment 3: clover-shaped trajectory

Experiment 3 aims to verify the robot's end-effector control capability along a more complex trajectory - clover-shaped path. The trajectory center is set at $I = [590\ 0\ 599]^T$(units: mm). To ensure continuous and precise motion, the trajectory is divided into 360 small steps, with a 1-second interval between steps.

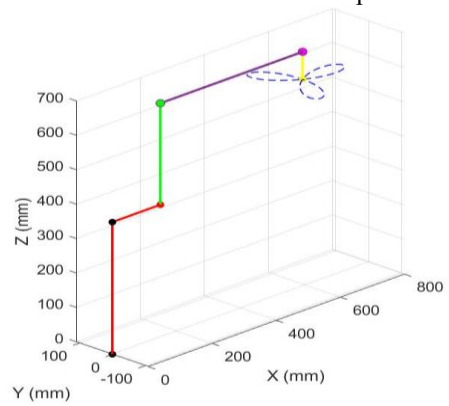

a. Clover-shaped trajectory simulation

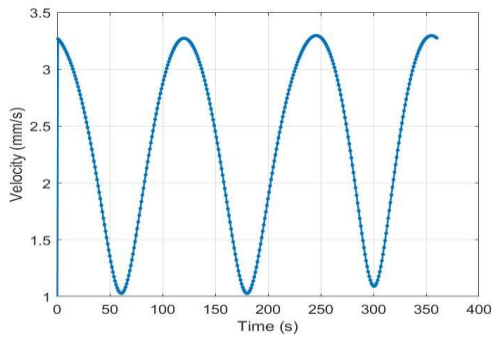

b. End-effector velocity variation chart for clover-shaped trajectory (image adjusted)

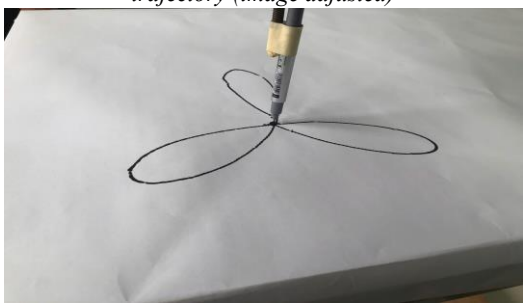

c. Actual clover-shaped motion of the end-effector

Figure 4. *Clover-shaped trajectory of the end-effector*

Simulation results of the control process are shown in Figure 4a. The end-effector velocity chart throughout trajectory execution is presented in Figure 4b. The results indicate that with evenly spaced trajectory steps, the end-effector velocity remains stable throughout the motion.

Figure 4c illustrates the experimental results for the robot executing the clover-shaped trajectory. After three repetitions, the end-effector closely followed the established trajectory with negligible deviation, demonstrating the feasibility and effectiveness of the proposed control method for nonlinear geometric paths. The clover-shaped trajectory records a radius error of $R = \pm 10\ mm$. The average velocity during execution is approximately $v_{tb} = 2.32\ mm/s$.

3.4. Comparison with previous studies

Compared to previous studies, the authors in [9] applied the Jacobian matrix to calculate velocity and identify singular configurations of planar parallel robots. However, this work was limited to simulation and algorithm development. Similarly, the research group in [10] proposed a trajectory planning method for SCARA robots to eliminate singular points and optimize the motion path, but only implemented on a simulation platform. Additionally, study [11] developed a torque controller based on the Jacobian matrix and optimized trajectories using genetic algorithms, but the results were also confined to simulating different trajectories.

Unlike these studies, this work proposes a velocity control solution for the end-effector using the Jacobian matrix and evaluates its effectiveness through both simulation and experimental validation. As a result, the research not only verifies the feasibility of the method but also demonstrates its high application potential in practical industrial manipulator control.

4. Conclusion

This study has presented a velocity kinematic control solution for industrial manipulators in palletizing applications. The system is built upon reconfiguring the 6-degree-of-freedom Motoman robot into a new configuration with four degrees of freedom, in which the end joint is fixed perpendicular to the ground to ensure stability during pick-and-place operations. Simplifying this structure not only reduces control complexity but also suits research conditions utilizing available hardware. Based on the new configuration, forward kinematics, inverse kinematics, and especially velocity kinematics models have been established using the Jacobian matrix. This approach enables accurate calculation of end-effector velocity based on joint velocities, thereby ensuring smooth and efficient motion within the workspace.

To evaluate the effectiveness of the proposed method, three experiments with different trajectory types - linear, circular, and clover-shaped - were conducted. Results from both simulation and experimental tests showed high consistency; notably, under experimental conditions, the manipulator's end-effector could accurately follow the entire predefined trajectory, confirming the feasibility and reliability of the proposed control solution.

The simulation and experimental results demonstrate high compatibility between the approaches, and confirm the capability for smooth and precise control of the end-effector along each trajectory. Thus, the study affirms the feasibility and effectiveness of the Jacobian-based velocity control solution for reconstructing controllers for industrial robots. Future research directions may include adjusting dynamic timing according to trajectory curvature, integrating real-time sensors, and expanding to flexible manufacturing environments.

REFERENCES

[1] S. Romero, *et al.* "Trajectory Planning for Robotic Manipulators in Automated Palletizing: A Comprehensive Review", *Robotics*, vol. 14, no. 5, p. 55, 2025, doi: 10.3390/robotics14050055.

[2] K. Nguyen-Vinh, H. Dewasurendra, S. Gonapaladeniya, U. Sarbahi, and N. Le, "Stack Algorithm Implementation in Robot-Based Mixed Case Palletizing System", in *Proc. 2022 4th Int. Conf. on Electrical, Control and Instrumentation Engineering (ICECIE)*, Kuala Lumpur, Malaysia, 26 Nov. 2022, pp. 1–8.

[3] A. Baldassarri, G. Innero, R. Di Leva, G. Palli, and M. Carricato, "Development of a mobile robotized system for palletizing applications", in *Proc. 2020 25th IEEE Int. Conf. on Emerging Technologies and Factory Automation (ETFA)*, Vienna, Austria, 8–11 Sept. 2020, vol. 1, pp. 395–401.

[4] F. Parisi, A. M. Mangini, and M. P. Fanti, "Optimal trajectory planning for a robotic manipulator palletizing tasks", in *Proc. 2020 IEEE Int. Conf. on Systems, Man, and Cybernetics (SMC)*, Toronto, ON, Canada, 11–14 Oct. 2020, pp. 2901–2906.

[5] S. D. Han, S. W. Feng, and J. Yu, "Toward Fast and Optimal Robotic Pick-and-Place on a Moving Conveyor", *IEEE Robotics and Automation Letters*, vol. 5, no. 2, pp. 446–453, Apr. 2020, doi: 10.1109/LRA.2019.2961605.

[6] V. T. Yen, B. V. Huy, and P. T. Van, "Design of adaptive robust controller based on neural networks control for industrial robot manipulator", (in Vietnamese) *The University of Danang - Journal of Science and Technology*, vol. 18, no. 11, pp. 21–26, Nov. 2020.

[7] N. X. Vinh, "Dynamics Analysis and optimization of the AKB Hybrid Palletizing Robot", (in Vietnamese) in *Proceedings of the 8th International Conference on Mechatronics Technology – VCM*, 2016.

[8] M. W. Spong, S. Hutchinson, and M. Vidyasagar, *Robot Modeling and Control*. Hoboken, NJ, USA: John Wiley & Sons, 1989.

[9] Q. T. Duong and D. T. Le, " Kinematics and singularity analysis of 3 degree-of-freedom planar parallel robotic manipulators", (in Vietnamese), *The University of Danang - Journal of Science and Technology,* vol 5, no 114, pp 76-80, 2017.

[10] N. V. Dim, T. X. Trong, B. V. Tung, L. H. Linh, and T.T. Ha, "Design and manufacturing of 4-DOF RPRR scara robot integrated identification of singular configuration", (in Vietnamese), *TNU Journal of Science and Technology*, vol. 229, no. 02, pp. 45-52, 2024.

[11] H. T. Luu and A. T. P. Nguyen, "Planning the optimal trajectory for a robotic manipulator using genetic algorithm", (in Vietnamese), *The University of Danang - Journal of Science and Technology,* Vol 20, no 4, pp 74-79, 2022.